



**HAL**  
open science

## Composition and density stratification observed by supercam in the first 300 sols in Jezero crater

R.C. Wiens, A. Udry, N. Mangold, O. Beyssac, C. Quantin, V. Sautter, A. Cousin, A. Brown, T. Bosak, L. Mandon, et al.

### ► To cite this version:

R.C. Wiens, A. Udry, N. Mangold, O. Beyssac, C. Quantin, et al.. Composition and density stratification observed by supercam in the first 300 sols in Jezero crater. 53rd Lunar and Planetary Science Conference, Mar 2022, En ligne, United States. pp.#2075. hal-03842432

**HAL Id: hal-03842432**

**<https://hal.science/hal-03842432v1>**

Submitted on 7 Nov 2022

**HAL** is a multi-disciplinary open access archive for the deposit and dissemination of scientific research documents, whether they are published or not. The documents may come from teaching and research institutions in France or abroad, or from public or private research centers.

L'archive ouverte pluridisciplinaire **HAL**, est destinée au dépôt et à la diffusion de documents scientifiques de niveau recherche, publiés ou non, émanant des établissements d'enseignement et de recherche français ou étrangers, des laboratoires publics ou privés.

**COMPOSITION AND DENSITY STRATIFICATION OBSERVED BY SUPERCAM IN THE FIRST 300 SOLS IN JEZERO CRATER.** R.C. Wiens<sup>1,2</sup>, A. Udry<sup>3</sup>, N. Mangold<sup>4</sup>, O. Beyssac<sup>5</sup>, C. Quantin<sup>6</sup>, V. Sautter<sup>5</sup>, A. Cousin<sup>7</sup>, A. Brown<sup>8</sup>, T. Bosak<sup>9</sup>, L. Mandon<sup>10</sup>, O. Forni<sup>7</sup>, J.R. Johnson<sup>11</sup>, S. McLennan<sup>12</sup>, C. Legett IV<sup>1</sup>, S. Maurice<sup>7</sup>, L. Mayhew<sup>13</sup>, L. Crumpler<sup>14</sup>, R.B. Anderson<sup>15</sup>, S.M. Clegg<sup>1</sup>, A.M. Ollila<sup>1</sup>, J. Hall<sup>9</sup>, P.-Y. Meslin<sup>7</sup>, L.C. Kah<sup>16</sup>, T.S.J. Gabriel<sup>15</sup>, P. Gasda<sup>1</sup>, J.I. Simon<sup>30</sup>, E.M. Hausrath<sup>32</sup>, B. Horgan<sup>2</sup>, F. Poulet<sup>17</sup>, P. Beck<sup>29</sup>, S. Gupta<sup>18</sup>, B. Chide<sup>1</sup>, E. Clavé<sup>19</sup>, S. Connell<sup>20</sup>, E. Dehouck<sup>6</sup>, G. Dromart<sup>6</sup>, T. Fouchet<sup>10</sup>, C. Royer<sup>10</sup>, J. Frydenvang<sup>21</sup>, O. Gasnault<sup>7</sup>, E. Gibbons<sup>22</sup>, H. Kalucha<sup>23</sup>, N. Lanza<sup>1</sup>, J. Lasue<sup>7</sup>, S. Le Mouelic<sup>6</sup>, R. Leveillé<sup>22</sup>, E. Cloutis<sup>19</sup>, G. Lopez Reyes<sup>24</sup>, G. Arana<sup>25</sup>, K. Castro<sup>25</sup>, J.M. Madariaga<sup>25</sup>, J.-A. Manrique<sup>24</sup>, C. Pilorget<sup>17</sup>, P. Pinet<sup>7</sup>, J. Laserna<sup>26</sup>, S.K. Sharma<sup>27</sup>, T. Acosta-Maeda<sup>27</sup>, E. Kelly<sup>27</sup>, F. Montmessin<sup>31</sup>, W. Fischer<sup>23</sup>, R. Francis<sup>28</sup>, K. Stack<sup>28</sup>, K. Farley<sup>23</sup>, and SuperCam Team<sup>1</sup>LANL (rwiens@lanl.gov), <sup>2</sup>Purdue, <sup>3</sup>UNLV, <sup>4</sup>LPG Nantes, <sup>5</sup>UPMC Paris, <sup>6</sup>U. Lyon, <sup>7</sup>IRAP Toulouse, <sup>8</sup>Plancius Res., <sup>9</sup>MIT, <sup>10</sup>LESIA Meudon, <sup>11</sup>APL/JHU, <sup>12</sup>Stony Brook U., <sup>13</sup>UC Boulder, <sup>14</sup>NM Museum of Natural History, <sup>15</sup>USGS Flagstaff, <sup>16</sup>UT Knoxville, <sup>17</sup>IAS Orsay, <sup>18</sup>Imperial College London, <sup>19</sup>U. Bordeaux, <sup>20</sup>U. Winnipeg, <sup>21</sup>Paris Obs. Meudon, <sup>22</sup>McGill U., <sup>23</sup>Caltech, <sup>24</sup>U. Valladolid, <sup>25</sup>U. Basque Country, <sup>26</sup>U. Malaga, <sup>27</sup>U. Hawaii, <sup>28</sup>JPL/Caltech, <sup>29</sup>U. Grenoble, <sup>30</sup>NASA/JSC, <sup>31</sup>LATMOS Guyancourt, <sup>32</sup>UNLV

**Introduction:** The Perseverance rover has traveled > 2.5 km since leaving its Octavia Butler landing site in Jezero crater ~300 sols ago. The SuperCam remote-sensing instrument suite has made > 1000 observations of bedrock along the traverse to provide a comprehensive picture of Jezero crater floor's chemistry and mineralogy. SuperCam combines high-resolution imaging, visible and near-infrared (VISIR) reflectance spectroscopy (0.4-0.85, 1.3-2.6  $\mu\text{m}$ ), remote time-resolved green-laser Raman and fluorescence spectroscopy, laser-induced breakdown spectroscopy (LIBS), and acoustic sensing into a single co-boresighted package [1, 2]. Derivation of the major-element abundances as oxide wt% for this part of the mission is presented in [3], while calibration of the VIS and IR spectrometers are given in [4-7].

Perseverance landed ~2 km from the Jezero crater delta front [8] on a unit that covers a large portion of the crater floor and is mapped as crater floor fractured rough (Cf-fr) [9]. The landing occurred in the Mááz formation just east of a lighter-toned unit referred to by the team as "Séitah" (Fig. 1). From orbit, the Mááz formation, part of Cf-fr, displays high-Ca pyroxene signatures, while olivine signatures dominate in Séitah [e.g., 10]. As shown in Fig. 1, the rover went S in the Mááz fm until Sol ~170, when it rounded the southern tip of Séitah. From there it drove NW along Artuby ridge before entering Séitah, where it is at the time of writing.

Targets at the landing site had granular texture, and the LIBS beam (~350  $\mu\text{m}$ ) interrogated single crystals in many cases, indicating that grain sizes were often 0.5 mm or larger. Two predominant morphologies were visible: flat "pavers" and high-standing rocks including topographic highs.

The first clear layering was observed at Mure, near the south end of Artuby ridge (Fig. 1) and the ridge itself consisted of massive rocks and some layers dipping downward away from Séitah; dipping was also observed in the subsurface by RIMFAX observations [11]. Based on this, the original vertical sequence likely consisted of Mááz fm as the uppermost, with Artuby ridge possibly

below it, and Séitah below both of them. Perseverance observed the units in that order.

**Increasingly Mafic Compositions:** Initial compositions at the landing site were generally basaltic to basaltic andesite. Chemical mixing trends indicate the dominant mineralogy contains plagioclase(-like), pyroxene (opx and augite), and iron oxides. High-standing rocks were overall slightly more felsic than pavers. As the rover drove southward and closer to Séitah (Fig. 1), it encountered fewer high-standing rocks and more pavers. Fig. 2 shows the compositional trend vs. sol#. More details of Mááz compositions are in [12].

Observations along Artuby ridge indicated a change in composition to higher Ca and Ti suggesting more augite (Fig. 2; Table 1). This was unexpected, as Artuby was mapped as part of Mááz. Olivine was not observed in Mááz, including Artuby. A pair of targets between Artuby ridge and the main part of Séitah were high in Mg and showed VISIR spectra indicating olivine (e.g., Entrevaux in Fig. 1), and as soon as Perseverance entered Séitah on Sol 202, LIBS, Raman, and VISIR all indicated olivine in coarse grained rocks (Figs. 3-4).

**Alteration and Interpretation:** SuperCam observed alteration products at low abundances, including Fe hydroxides, Mg sulfates, Mg-Fe carbonates, and Na perchlorates in Mááz, and Mg-Fe carbonates and Mg sulfates in Séitah. These alteration products result in low major-element totals because volatiles such as S, H, C, and Cl are not quantified in the elemental composition, and they are discussed in several other presentations [13]. Chemical compositions do not indicate enrichment of Al as would be expected from open system weathering to Al phyllosilicates. Our interpretation, based on textures and compositions, is that all of the materials sampled so far are igneous with mild to moderate degrees of aqueous alteration, e.g., from Jezero Lake which likely overlaid these materials for part of their history, and subsequent groundwater.

**Density and Compositional Stratification:** By removing observations with low major-element totals (indicating alteration) and normalizing the remaining compositions, a clear density gradient is observed from

Mááz through Artuby to Seitah as shown in Table 1. The Mg # of Séitah’s olivines (not shown here) indicate that they are out of equilibrium with the bulk material. Our preliminary interpretation is that Seitah is an igneous cumulate. Decreasing density with successive overlying materials could suggest that all units are part of the same magma body, or that more evolved magma was erupted near the surface after emplacement of Seitah.

Olivine-rich materials capped by less mafic material are characteristic of the Nili-Syrtis region surrounding and to the west of Jezero crater [14]. Perseverance is expected to traverse many of these materials including those outside of Jezero crater. Observations and samples acquired during the traverse in and beyond the crater should reveal much more about igneous and aqueous activity that modified the terrain in this region.

**Acknowledgments:** We are grateful to the many engineers and scientists who have supported the Perseverance mission. We acknowledge the support of NASA’s Mars Exploration Program, CNES, CNRS, and other supporting organizations. SuperCam data are archived in the PDS.

**References:** [1] S. Maurice et al. (2021) *Spa. Sci. Rev.* 217, 47. [2] R.C. Wiens et al. (2021) *SSR* 217, 4. [3] R.B. Anderson et al. (2021) *Spectrochim. Acta B*, accepted. [4] C. Royer et al. (2020) *Rev. Sci. Instrum.* 91, 063105. [5] C. Royer et al. (2022) this meeting. [6] C. Legett et al. (2022) *subm. to Appl. Optics*. [7] C. Legett et al. (2022) this meeting. [8] N. Mangold et al. (2021) *Science* 10.1126/science.aba4051. [9] Stack et al. (2021) *SSR* 217, 127. [10] B. Horgan et al. (2020) *Icarus* 339, 113526. [11] P. Russell et al. (2022) this meeting. [12] A. Udry et al. (2022) this meeting. [13] L. Mandon et al., P. Beck et al., P.-Y. Meslin et al., F. Poulet et al. (2022), all at this meeting. [14] T. Goudge et al. (2015) *JGRP* 120, 10.1002/2014JE004782.

Table 1. CIPW norms, Mg#, and densities calculated from LIBS for the three units traversed by Perseverance.

Wt%	Mááz fm	Artuby	Séitah fm
Plagioclase	37.9	30.0	15.2
Orthoclase	7.1	3.6	1.2
Diopside	4.8	16.7	1.5
Hypersthene	37.9	41.5	34.7
Olivine	0.0	0.9	41.1
Mg #	19.3	21.1	62.8
Density (g/cc)	3.10(.02)	3.27(.03)	3.37(.01)

Numbers in parentheses are propagated error from the standard deviation of the mean elemental composition

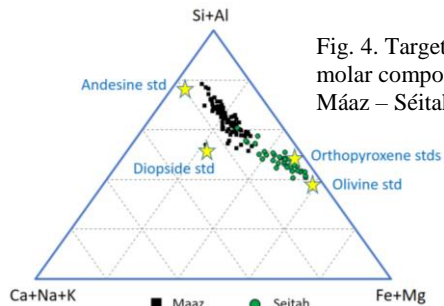


Fig. 4. Target-averaged molar compositions show Mááz – Séitah differences.

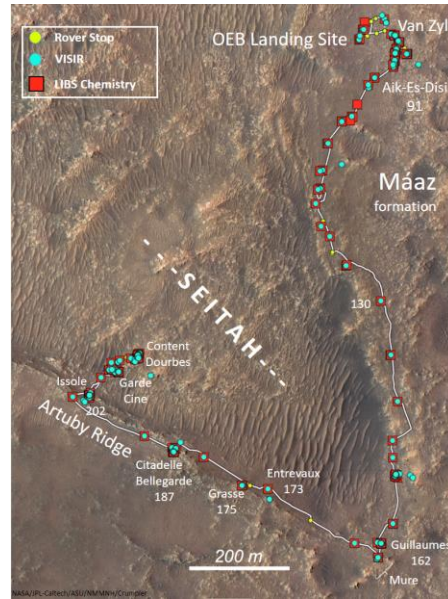


Fig. 1. Map of traverse showing locations of SuperCam observations, sol numbers, and features mentioned in the text.

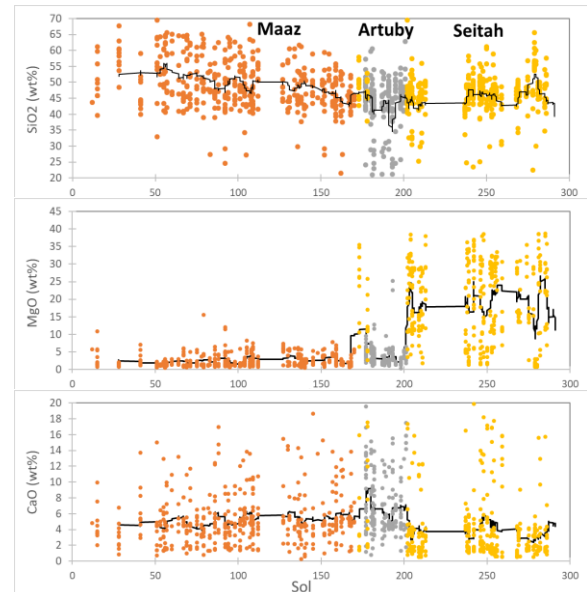


Fig. 2. LIBS bedrock observations along the traverse for selected elements along with 30-point running average.

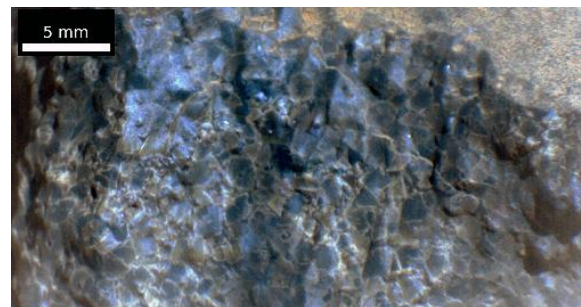


Fig. 3. Color-stretched SuperCam image of Séitah target Cine with angular 1.5 mm olivine grains.